Hindawi Publishing Corporation
Journal of Nanomaterials
Volume 2012, Article ID 648012, 6 pages
doi:10.1155/2012/648012

Research Article

Preparation and Characterization of $Ni(OH)_2$ and NiO Mesoporous Nanosheets

Changyu Li and Shouxin Liu

College of Material Science and Engineering, Northeast Forestry University, Harbin 150040, China

Correspondence should be addressed to Shouxin Liu, liushouxin@126.com

Received 30 July 2011; Revised 30 September 2011; Accepted 30 September 2011

Academic Editor: Bo Zou

Mesoporous nanosheets of single-crystalline β-nickel hydroxide (β-$Ni(OH)_2$) were successfully synthesized via a facile hydrothermal method using $Ni(NO_3)_2 \cdot 6H_2O$ as precursor in a mixed solution of sodium hydroxide (NaOH) and sodium dodecylbenzenesulfonate (SDBS). Single-crystalline nickel oxide (NiO) mesoporous nanosheets can be obtained through a thermal decomposition method using β-$Ni(OH)_2$ mesoporous nanosheets as precursor. The influences of SDBS and hydrothermal treatment were carefully investigated; the results showed that they played important roles in the formation of β-$Ni(OH)_2$ mesoporous nanosheets. The as-obtained β-$Ni(OH)_2$ and NiO were characterized by X-ray diffraction (XRD), transmission electron microscopy (TEM), thermal gravity-differential thermal analysis (TG-DTA), and specific surface area, and pore size test.

1. Introduction

The development of nanomaterials is attracting increasing attentions due to their unique physical and chemical properties that are different from conventional bulk materials. It is well known that the size, morphology, and structure of nanomaterials significantly influence their physical and chemical properties and, therefore, their applications [1–3]. The nanomaterials with mesoporous structures Especially have technical advances in various fields, such as adsorption, separation, catalysis, drug delivery, sensors, photonics, and nanodevices [4, 5].

As reported, nickel hydroxide ($Ni(OH)_2$) has attracted increasing interests due to its applications in alkaline rechargeable batteries (such as Ni/MH, Ni/Zn, Ni/Cd, and Ni/Fe, [6–8]), which are most widely used in many applications ranging from power tools to portable electronics and electric vehicles [9]. There are two phases of $Ni(OH)_2$, known as α-$Ni(OH)_2$ and β-$Ni(OH)_2$. Single-crystalline β-$Ni(OH)_2$ nanosheets have been demonstrated taking advantage of its intrinsic lamellar structure [9–11] and widely used due to its high stacking density and stability in alkaline condition compared with α-$Ni(OH)_2$. Recently, some reports have demonstrated that $Ni(OH)_2$ with a smaller crystalline size and more crystalline defects possesses a higher chemical proton diffusion coefficient, and this will diminish the concentration polarization of protons during charge/discharge cycle, leading to a better charge/discharge cycling behavior [12]. Literatures have reported that the activity of $Ni(OH)_2$ electrode could be significantly improved when nanosized $Ni(OH)_2$ was added into microsized $Ni(OH)_2$ [13, 14]; especially, nanosized $Ni(OH)_2$ with mesoporous structures can enhance the electrochemical performance greatly [15]. Furthermore, NiO is a very important p-type semiconductor with a direct band gap of 3.5 eV and often used as catalyst, electrochemical capacitor, fuel cell electrode, gas sensor, and so forth [16–18]. NiO can be obtained by calcinating the corresponding $Ni(OH)_2$ simply in air, and the shape of $Ni(OH)_2$ particles could be maintained [19]. To date, numerous works [20–24] have been developed to synthesize $Ni(OH)_2$ with different morphologies because the electrochemical performances of $Ni(OH)_2$ are directly affected by its morphology and size [25–27]. Chen and Gao [10] reported the synthesis of different morphologies of nickel hydroxide through using ethanol as growth media. Meyer et al. [11] synthesized platelet-like nanoparticles of nickel hydroxide. Matsui et al. [28] obtained $Ni(OH)_2$ nanorods using carbon-coated anodic alumina film in hydrothermal

conditions. However, to obtain well-defined $Ni(OH)_2$ nanostructures with mesoporous structure is still the challenge in nanochemistry and nanomaterials.

Herein, we demonstrate a facile method for the synthesis of single-crystal β-$Ni(OH)_2$ mesoporous nanosheets, and NiO mesoporous nanosheets can also be obtained through the thermal decomposition using the as-prepared β-$Ni(OH)_2$ as precursor.

2. Experimental

All of the reagents, except SDBS (chemical purity), were of analytical grade and used as received without further purification. In a typical experiment, 0.370 g $Ni(NO_3)_2 \cdot 6H_2O$ and 0.930 g SDBS were dissolved in 80 mL distilled water under magnetic stirring for 15 min to form a homogeneous solution at room temperature, and then 0.170 g NaOH was added into the solution. Afterward, the solution was transferred into a 100 mL Teflon-lined stainless autoclave, sealed and maintained at 140°C for 24 h, and then cooled to room temperature naturally. The products were collected, washed several times with distilled water and absolute ethanol, and dried at 60°C in air. To study the influences of SDBS and hydrothermal treatment on the formation of β-$Ni(OH)_2$ nanosheets, parallel experiments were carried out with keeping other reaction conditions unchanged.

As-prepared β-$Ni(OH)_2$ was calcined in air at 400°C for 2 h to produce NiO.

X-ray diffraction (XRD) patterns of the prepared samples were recorded on a D/max-r B X-ray diffractometer with graphite-monochromatized CuKα radiation (λ = 1.5418 Å), employing a scanning rate of 4°/min in the range from 15° to 90°. The size and morphology of the products were characterized by H-7650 transmission electron microscopy (TEM). High-resolution transmission electron microscopy (HRTEM, Tecnai F30) with the selected area of electron-diffraction (SAED) was employed to investigate the detailed structure of β-$Ni(OH)_2$ microstructures. The N_2 adsorption-desorption isotherms and Barrett-Joyner-Halenda (BJH) pore size distribution were investigated on a Micromeritics ASAP 2020 equipment. TG-DSC (a Pyris Diamond thermogravimetric/DSC apparatus) was used to analyze the thermal behavior of samples with a heating rate of 10°C/min from room temperature to 600°C in air.

3. Results and Discussion

In Figure 1, curve (a) shows the XRD pattern of β-$Ni(OH)_2$ prepared by the typical method. All diffraction peaks can be indexed to the pure hexagonal phase of β-$Ni(OH)_2$ (JCPDS, file No. 14-0117). No peaks from impurities are observed, indicating that the product was pure phase. Curve (b) shows the XRD pattern of the β-$Ni(OH)_2$ sample prepared in the absence of SDBS, from which, it is obvious to see the intensity change of some peaks compared with curve (a). Curve (c) is the XRD pattern of $Ni(OH)_2$ prepared at room temperature. As shown, the Bragg reflections are broad, indicating that this sample has small size and poor

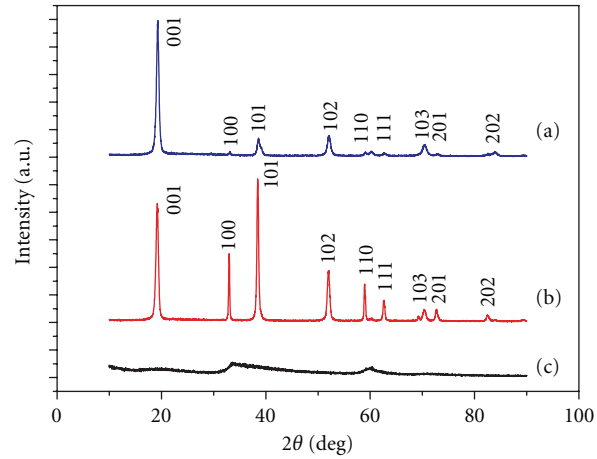

Figure 1: XRD patterns of the prepared β-$Ni(OH)_2$ samples: (a) with using SDBS; (b) without using SDBS; (c) without hydrothermal treatment.

crystallinity. According to curve (a) and curve (c), it proves that hydrothermal treatment plays an important role in improving their crystallinity. This result is consistent with the literature [29, 30].

As known, the morphology and size of nanoparticles prepared by hydrothermal methods could be well-controlled by the addition of certain surfactant. Many theories have also been proposed to describe the mechanism of the shape-revolution process; however, they did not carry much conviction. From the difference between curve (a) and (b) in Figure 1, it can be concluded that all diffraction peak directions, except for [001] direction, are suppressed with the addition of SDBS. In other words, the prepared β-$Ni(OH)_2$ has a preferential [001] growth direction in the presence of SDBS. It is well known that the surfactant in solution will aggregate into micelles. During the reaction, the micelles play the roles of "seeds;" the originally produced clusters will aggregate on the micelles, and further grow to nanoproducts, which can be called a special soft template technique to synthesize nanowires [31]. In our case, this process slows down the reaction rate of Ni^{2+} and OH^- and determines the preferential growth direction of β-$Ni(OH)_2$ nanoparticles.

Figure 2 shows the TEM images of the β-$Ni(OH)_2$ products obtained from different reaction conditions. As indicated in Figure 2(a), the obtained β-$Ni(OH)_2$ products are irregular hexagonal shapes with sharp edges and the edge sizes are in the range of 25–160 nm. The rod-like structures are formed because of some sheets being on edge in the grid. Figure 2(b) shows the TEM image of β-$Ni(OH)_2$ nanosheets prepared without the presence of SDBS, indicating the smaller size. Figure 2(c) shows the product obtained without the hydrothermal treatment, from which we can see that the sample has an irregular shape and a poor crystallized structure. The results indicate that hydrothermal treatment plays an important role in the formation of β-$Ni(OH)_2$ nanosheets; coinciding with the literature [32].

Figure 3(a) gives the magnified TEM image of the β-$Ni(OH)_2$ nanosheets, the bright spots on the surface of

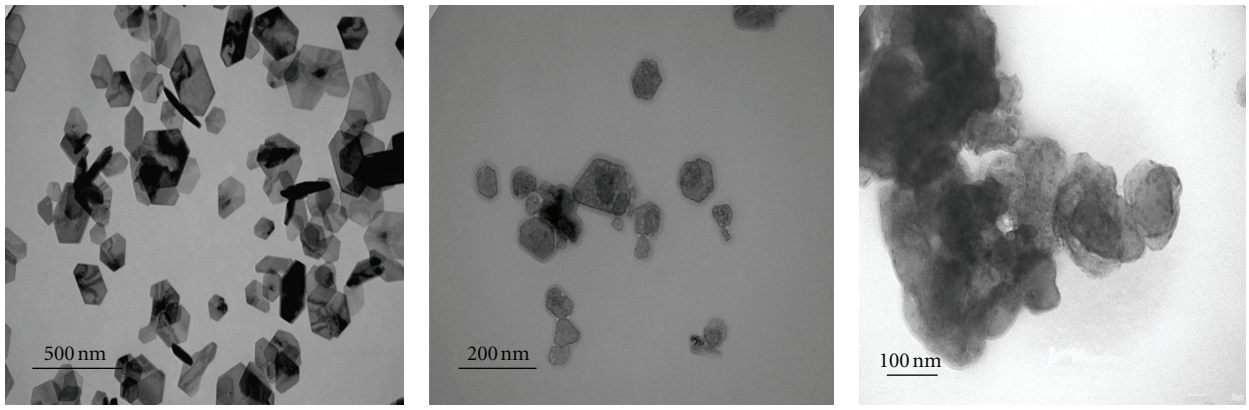

(a) (b) (c)

Figure 2: TEM images of the β-Ni(OH)$_2$ nanosheets prepared: (a) in the presence of SDBS, (b) without using SDBS, and (c) without hydrothermal treatment.

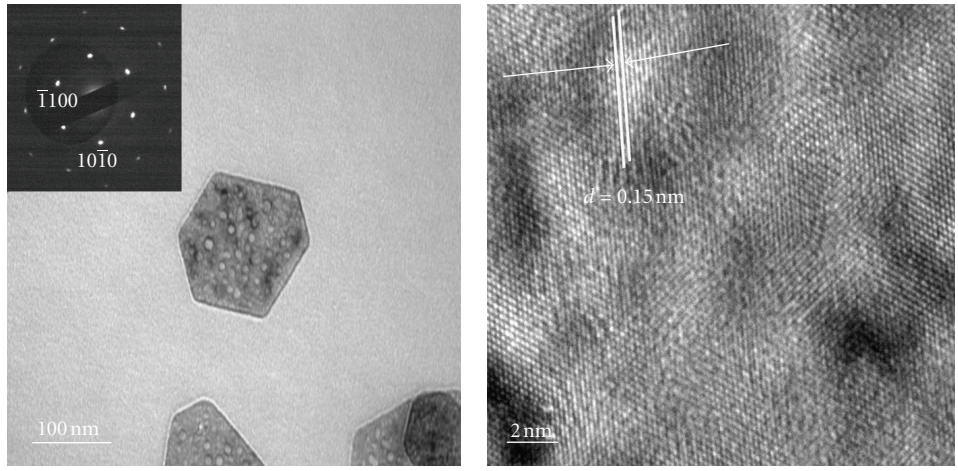

(a) (b)

Figure 3: (a) TEM and (b) HRTEM images of β-Ni(OH)$_2$ mesoporous nanosheets. Inset of (a) is the corresponding SAED pattern.

the sheets reveal the porous structure. As shown in SEAD pattern (inset of Figure 3(a)), the as-prepared β-Ni(OH)$_2$ nanosheets are single crystals of hexagonal phase, and the surfaces of these hexagonal β-Ni(OH)$_2$ nanosheets are the (001) planes. Figure 3(b) exhibits the HRTEM image of the β-Ni(OH)$_2$ nanosheets, from which we can see that the crystal lattice planes are perfectly aligned. The lattice space of about 1.50 Å corresponds to the interplanar spacing of (003) planes, indicating that the β-Ni(OH)$_2$ nanosheets have a preferential [001] growth direction, consistent with the result of XRD as well.

The thermal property of the β-Ni(OH)$_2$ nanosheets was analyzed by TG-DSC, and the variations of heat and weight while β-Ni(OH)$_2$ was being sintered are recorded. As shown in Figure 4, there is an endothermic peak at 336.2°C in the DSC curve, accompanied by a weight loss of 18.81% (observed in TG curve at the same temperature), resulting from the thermal decomposition of β-Ni(OH)$_2$. When β-Ni(OH)$_2$ sample was heated to above 336.2°C, we can not observe any obvious endothermic or exothermic peak in the DSC curve. The slight mass change between 336.2 and 500°C is due to the desorption of oxygen from bulk NiO, and we can conclude that β-Ni(OH)$_2$ precursor could be decomposed to NiO above 336.2°C completely. The observed weight loss of 18.81% is close to the calculated loss value of 19.4%.

Based on the TG and DSC results, in our experiments, the as-prepared β-Ni(OH)$_2$ nanosheets were calcined at 400°C for 2 h to obtain NiO nanosheets. Figure 5 gives the XRD pattern of NiO powder. All the diffraction peaks can be indexed to a face-centered cubic phase NiO with lattice parameters $a = 4.17$ (JCPDS, file No. 78-0643), and no diffraction peaks of Ni(OH)$_2$ or other impurities were observed, indicating that β-Ni(OH)$_2$ has been converted to NiO completely.

The size and morphology of the as-prepared NiO were examined by TEM. Figure 6(a) exhibits the TEM image of NiO, showing that the shape of nanosheets was maintained after the thermal decomposition of β-Ni(OH)$_2$. The

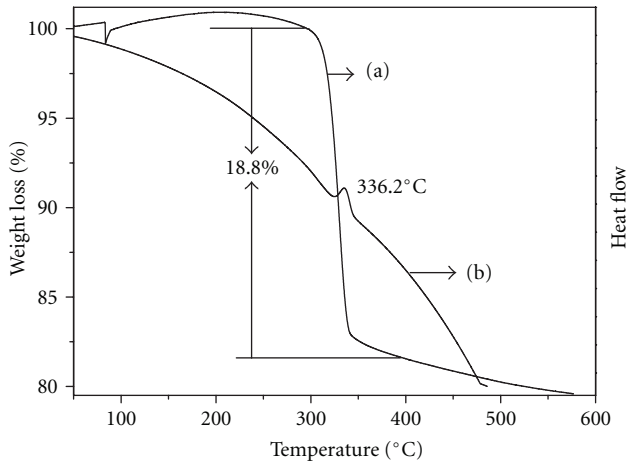

Figure 4: TG-DSC curves of β-Ni(OH)$_2$ mesoporous nanosheets.

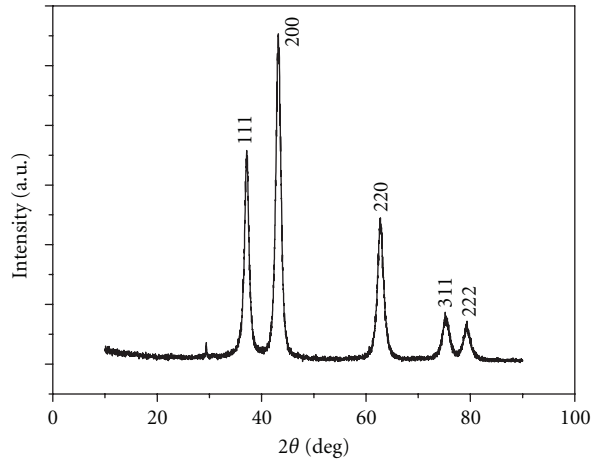

Figure 5: XRD pattern of the NiO mesoporous nanosheets.

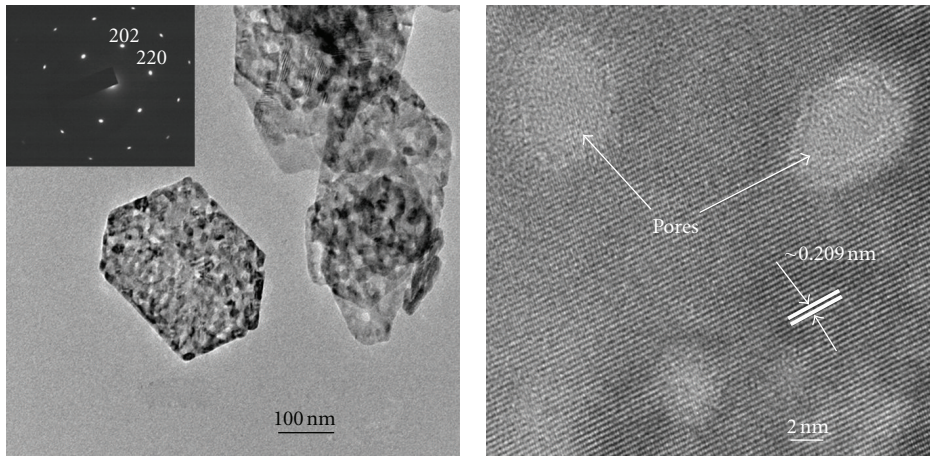

(a) (b)

Figure 6: (a) TEM and (b) HRTEM images of NiO mesoporous nanosheets. Inset of (a) is the corresponding SAED pattern.

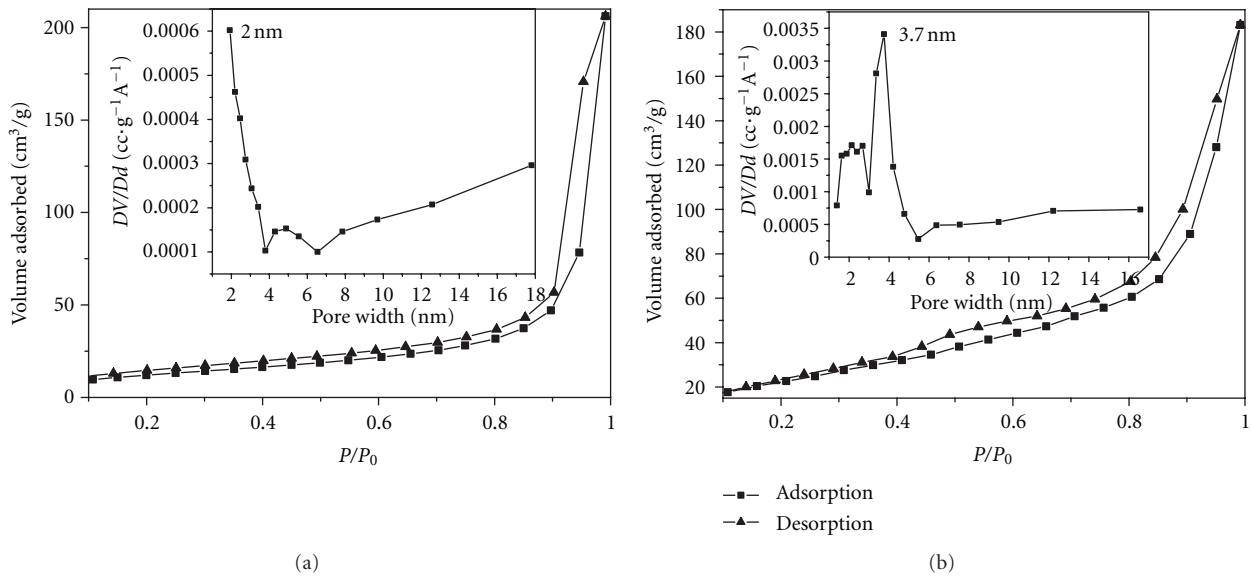

Figure 7: N_2 adsorption-desorption isotherm and pore size distribution (insets) of (a) β-$Ni(OH)_2$ and (b) NiO nanosheets.

corresponding SAED pattern of NiO nanosheets (inset in Figure 6(a)) exhibits many spots, indicating the nature of single crystal. The diffraction pattern can be indexed to the face-centered cubic NiO, consistent with the XRD result. Figure 6(b) is the HRTEM image of the as-prepared NiO nanosheets. As shown in it, the crystal lattice planes are perfectly aligned, and the lattice space is about 2.09 Å, corresponding to the interplanar spacing of 200 planes for cubic NiO. This reveals that the growth of the nanosheets follows the 200 direction; in other words, the nanosheets grow along with the *a* axis.

TEM images of β-$Ni(OH)_2$ and NiO (Figure 3(a) and Figure 6(a)) reveal their mesoporous structure by the wormhole-like porous structure on the surfaces of the sheets, then the mesoporous structures and pore sizes of β-$Ni(OH)_2$ and NiO were investigated by the N_2 adsorption/desorption techniques. The N_2 adsorption-desorption isotherms and BJH pore size distribution profiles (inset in Figures 7(a) and 7(b)) of β-$Ni(OH)_2$ and NiO were shown in Figure 7. It is obvious that these isotherms can be closely related to IV-type isotherm, characteristic of mesoporous materials. The BET surface area of mesoporous β-$Ni(OH)_2$ nanosheets is 46.6 $m^2\,g^{-1}$, and the pore size distribution is peaked at around 2 nm (inset in Figure 7(a)). For NiO mesoporous nanosheets (mesoporous $Ni(OH)_2$ calcinated at 400°C for 2 h), the BET surface areas and the pore size distribution increase to 85.98 $m^2\,g^{-1}$ and 3.7 nm, respectively.

4. Conclusion

In summary, a progressive production of β-$Ni(OH)_2$ mesoporous nanosheets with single-crystalline structure has been constructed via a one-step SDBS-assisted hydrothermal route. Using the obtained β-$Ni(OH)_2$ nanosheets as precursors, NiO nanosheets could be obtained by the calcination at 400°C for 2 h. The results of some parallel experiments show that surfactant SDBS and hydrothermal treatment have important effect on the formation of β-$Ni(OH)_2$ nanosheets. The N_2 adsorption/desorption isotherms and BJH pore size distribution profiles of β-$Ni(OH)_2$ and NiO confirm their mesoporous structure.

Disclosure

The paper is original and it has been written by the stated authors who are all aware of its content and approve its submission. It has not been published previously and is not under consideration for publication elsewhere.

Conflict of Interests

There is no conflict of interest exists in our paper.

Acknowledgment

This work is supported by the National Nature Science Fund of China Grant no. 30771692.

References

[1] Z. H. Kang, E. B. Wang, L. Gao et al., "One-step water-assisted synthesis of high-quality carbon nanotubes directly from graphite," *Journal of the American Chemical Society*, vol. 125, no. 45, pp. 13652–13653, 2003.

[2] S. Y. Lian, E. B. Wang, Z. H. Kang et al., "Synthesis of magnetite nanorods and porous hematite nanorods," *Solid State Communications*, vol. 129, no. 8, pp. 485–490, 2004.

[3] Z. B. Lei, G. J. Ma, M. Y. Liu et al., "Sulfur-substituted and zinc-doped in$(OH)_3$: a new class of catalyst for photocatalytic H_2 production from water under visible light illumination," *Journal of Catalysis*, vol. 237, no. 2, pp. 322–329, 2006.

[4] T. Kresge, M. E. Leonowicz, W. J. Roth, J. C. Vartuli, and J. S. Beck, "Ordered mesoporous molecular sieves synthesized by a liquid-crystal template mechanism," *Nature*, vol. 359, no. 6397, pp. 710–712, 1992.

[5] A. Navrotsky, O. Trofyrnluk, and A. Andrey, "Thermochemistry of microporous and mesoporous materials," *Chemical Reviews*, vol. 109, no. 9, pp. 3885–3902, 2009.

[6] W.-K. Hu and D. Noréus, "Alpha nickel hydroxides as lightweight nickel electrode materials for alkaline rechargeable cells," *Chemistry of Materials*, vol. 15, no. 4, pp. 974–978, 2003.

[7] X. M. He, J. J. Li, H. W. Cheng, C. Y. Jiang, and C. R. Wan, "Controlled crystallization and granulation of nano-scale β-$Ni(OH)_2$ cathode materials for high power Ni-MH batteries," *Journal of Power Sources*, vol. 152, no. 1-2, pp. 285–290, 2005.

[8] W. G. Zhang, W. Q. Jiang, L. M. Yu, Z. Z. Fu, W. Xia, and M. L. Yang, "Effect of nickel hydroxide composition on the electrochemical performance of spherical Ni(OH)2 positive materials for Ni-MH batteries," *International Journal of Hydrogen Energy*, vol. 34, no. 1, pp. 473–480, 2009.

[9] Z. H. Liang, Y. J. Zhu, and X. L. Hu, "β-nickel hydroxide nanosheets and their thermal decomposition to nickel oxide nanosheets," *Journal of Physical Chemistry B*, vol. 108, no. 11, pp. 3488–3491, 2004.

[10] D. L. Chen and L. Gao, "A new and facile route to ultrafine nanowires, superthin flakes and uniform nanodisks of nickel hydroxide," *Chemical Physics Letters*, vol. 405, no. 1–3, pp. 159–164, 2005.

[11] M. Meyer, A. Bée, D. Talbot et al., "Synthesis and dispersion of $Ni(OH)_2$ platelet-like nanoparticles in water," *Journal of Colloid and Interface Science*, vol. 277, no. 2, pp. 309–315, 2004.

[12] M. C. Bernard, R. Cortes, M. Keddam, H. Takenouti, P. Bernard, and S. Senyarich, "Structural defects and electrochemical reactivity of β-$Ni(OH)_2$," *Journal of Power Sources*, vol. 63, no. 2, pp. 247–254, 1996.

[13] X. J. Han, P. Xu, C. Q. Xu, L. Zhao, Z. B. Mo, and T. Liu, "Study of the effects of nanometer β-$Ni(OH)_2$ in nickel hydroxide electrodes," *Electrochimica Acta*, vol. 50, no. 14, pp. 2763–2769, 2005.

[14] X. H. Liu and L. Yu, "Influence of nanosized Ni(OH)2 addition on the electrochemical performance of nickel hydroxide electrode," *Journal of Power Sources*, vol. 128, no. 2, pp. 326–330, 2004.

[15] B. Li, M. Ai, and Z. Xu, "Mesoporous β-$Ni(OH)_2$: synthesis and enhanced electrochemical performance," *Chemical Communications*, vol. 46, no. 34, pp. 6267–6269, 2010.

[16] M. S. Wu and H. H. Hsieh, "Nickel oxide/hydroxide nanoplatelets synthesized by chemical precipitation for electrochemical capacitors," *Electrochimica Acta*, vol. 53, no. 8, pp. 3427–3435, 2008.

[17] J. J. He, H. Lindström, A. Hagfeldt, and S. E. Lindquist, "Dye-sensitized nanostructured p-type nickel oxide film as a photocathode for a solar cell," *Journal of Physical Chemistry B*, vol. 103, no. 42, pp. 8940–8943, 1999.

[18] X. F. Song and L. Gao, "Facile synthesis and hierarchical assembly of hollow nickel oxide architectures bearing enhanced photocatalytic properties," *Journal of Physical Chemistry C*, vol. 112, no. 39, pp. 15299–15305, 2008.

[19] M. H. Cao, X. Y. He, J. Chen, and C. W. Hu, "Self-assembled nickel hydroxide three-dimensional nanostructures: a nanomaterial for alkaline rechargeable batteries," *Crystal Growth & Design*, vol. 7, no. 1, pp. 170–174, 2007.

[20] D. N. Yang, R. M. Wang, M. S. He, J. Zhang, and Z. F. Liu, "Ribbon—and boardlike nanostructures of nickel hydroxide: synthesis, characterization, and electrochemical properties," *Journal of Physical Chemistry B*, vol. 109, no. 16, pp. 7654–7658, 2005.

[21] S. M. Zhang and H. Zeng, "Self-assembled hollow spheres of β-$Ni(OH)_2$ and their derived nanomaterials," *Chemistry of Materials*, vol. 21, no. 5, pp. 871–883, 2009.

[22] J. T. Sun, J. G. Cheng, C. W. Wang, X. L. Ma, M. Li, and L. J. Yuan, "Synthesis and morphological control of nickel hydroxide for lithium-nickel composite oxide cathode materials by an eddy circulating precipitation method," *Industrial and Engineering Chemistry Research*, vol. 45, no. 6, pp. 2146–2149, 2006.

[23] L. H. Dong, Y. Chu, and W. D. Sun, "Controllable synthesis of nickel hydroxide and porous nickel oxide nanostructures with different morphologies," *Chemistry—A European Journal*, vol. 14, no. 16, pp. 5064–5072, 2008.

[24] Q. Y. Li, R. N. Wang, Z. R. Nie, Z. H. Wang, and Q. Wei, "Preparation and characterization of nanostructured $Ni(OH)_2$ and NiO thin films by a simple solution growth process," *Journal of Colloid and Interface Science*, vol. 320, no. 1, pp. 254–258, 2008.

[25] X. Han, X. Xie, C. Xu, D. Zhou, and Y. Ma, "Morphology and electrochemical performance of nano-scale nickel hydroxide prepared by supersonic coordination-precipitation method," *Optical Materials*, vol. 23, no. 1-2, pp. 465–470, 2003.

[26] X. Y. Guan and J. C. Deng, "Preparation and electrochemical performance of nano-scale nickel hydroxide with different shapes," *Materials Letters*, vol. 61, no. 3, pp. 621–625, 2007.

[27] T. N. Ramesh, "Crystallite size effects in stacking faulted nickel hydroxide and its electrochemical behaviour," *Materials Chemistry and Physics*, vol. 114, no. 2-3, pp. 618–623, 2009.

[28] K. Matsui, T. Kyotani, and A. Tomita, "Hydrothermal synthesis of single-crystal Ni(OH)2 nanorods in a carbon-coated anodic alumina film," *Advanced Materials*, vol. 14, no. 17, pp. 1179–1219, 2002.

[29] M. H. Cao, T. F. Liu, S. Gao et al., "Single-crystal dendritic micro-pines of magnetic α-Fe_2O_3: large-scale synthesis, formation mechanism, and properties," *Angewandte Chemie International Edition*, vol. 44, no. 27, pp. 4197–4201, 2005.

[30] H. B. Liu, L. Xiang, and Y. Jin, "Hydrothermal modification and characterization of $Ni(OH)_2$ with high discharge capability," *Crystal Growth and Design*, vol. 6, no. 1, pp. 283–286, 2006.

[31] Y. K. Liu, Y. Chu, L. K. Yang, D. X. Han, and Z. X. Lü, "A novel solution-phase route for the synthesis of crystalline silver nanowires," *Materials Research Bulletin*, vol. 40, no. 10, pp. 1796–1801, 2005.

[32] Y. W. Li, Q. X. Yang, J. H. Yao, Z. G. Zhang, and C. J. Liu, "Effect of synthesis temperature on the phase structure and electrochemical performance of nickel hydroxide," *Ionics*, vol. 16, no. 3, pp. 221–225, 2010.